Strong Improper Ferroelasticity and Weak Canted Ferroelectricity in a Martensitic-Like Phase Transition of Diisobutylammonium Bromide

Anna Piecha-Bisiorek, Agata Białońska, Ryszard Jakubas, Piotr Zieliński, Martyna Wojciechowska, and Mirosław Gałązka*

Ferroelectricity of “small-molecule” organic compounds has been known for almost a century.[1–3] The technological applicability of such materials has not as yet reached the level of inorganic system-like perovskite-based ceramics, e.g., PZT (lead zirconate titanate)[4–8] that owe their attractiveness to a combination of various useful physical properties such as luminescence, superconductivity, and stable ferroelectricity. The advantages of organic ferroelectrics are, however, incontestable so that the synthesis and growth of new such systems are a challenging research area.

Recently synthesized environment-friendly and small-molecular-weight organic single- and two-components polar materials[9–21] turned out very promising. An excellent example of the single-component pure organic ferroelectric with a room-temperature ferroelectricity is croconic acid whose polar properties have been studied by Horiuchi et al.[11] The spontaneous polarization P_s of about 21 μC cm^{-2} and the coercive field of order of 14 kV cm^{-1} allows this material to successfully compete with the inorganic ferroelectric materials. Noteworthy is the crucial role of the hydrogen bonding and a specific cooperative proton tautomerism (the migration of a proton from the β position to the enol) in the onset of ferroelectricity in π-conjugated molecular compounds.

Other two-component organic ferroelectrics, diisopropylammonium chloride (DIPAC) and diisopropylammonium bromide (DIPAB), belong to the group of molecular-ionic compounds with the spontaneous polarization resulting from ordering organic cations (order–disorder-type ferroelectric). A particular behavior of their dielectric parameters (especially DIPAB) distinguishes them from the formerly reported organic, hydrogen-bonded ferroelectrics.[19–21] This compound is characterized by an extremely high value of the spontaneous polarization (23 μC cm^{-2}), a high Curie temperature (426 K), a high dielectric constant, small dielectric losses and a low coercivity field.[20,21] Additional qualities of DIPAB are: facility of preparation, low cost, nontoxicity, and good thermal stability. DIPAB also shows a strong piezoelectric effect and has a well-defined ferroelectric domain structure.

Numerous newly synthesized materials exhibit a symmetry-induced coupling of ferroelectricity to a macroscopic strain.[22,23] The materials fall, thus, into the category of biferroics (ferroelectric–ferroelastic).[24–26] In most cases, a spontaneous strain is a secondary order parameter. In this respect, diisobutylammonium bromide, (DIBAB), [i-$(C_4H_9)_2NH_2^+$][Br$^-$], presented in this paper, is unique, because the elastic degrees of freedom seem to play the essential role in the formation of a domain pattern that resembles that of martensitic phase transitions,[27] whereas the ferroelectricity appears as a side effect. The lack of a group–subgroup relation at the phase transition, a very strong spontaneous strain without cracking of the lattice makes the system even more intriguing and at the same time closer to martensitic materials.

DIBAB reveals thermal stability at a wide range of temperatures (up to about 450 K, see Figure S1, Supporting Information) and undergoes only one, reversible phase transition at 285/286 K (cooling/heating) as is presented in **Figure 1**a. A well-shaped heat anomaly as well as a thermal hysteresis (ΔT = 1 K) indicates the discontinuous (first order) character of this transition. The corresponding value of the transition entropy, ΔS = 25 J mol^{-1} K^{-1}, indicates that the room temperature phase is highly disordered. Structural data reveal an “order-disorder” underlying mechanism.

At room temperature (293 K), the symmetry of DIBAB is described by the tetragonal *I*4/*mmm* space group. The asymmetric unit contains a bromide anion and a half of the DIBA$^+$ cation with $-$CH(CH$_3$)$_2$ group disordered over two positions. The bromide anion occupies a special position 4/*mmm* whereas the amine N atom of the DIBA$^+$ cation is located in a vicinity of another special position 4/*mmm*. The methylene C atoms bonded to the amine N atom occupy the special positions 4*mm*, and the CH(CH$_3$)$_2$ groups bonded to the latter are placed in general positions. As a result, the amine N atom and the CH(CH$_3$)$_2$ groups exhibit four and sixteen positioned disorder, respectively (Figure 1-right). The structure of DIBAB is layered so that each bromide anion is surrounded by four DIBA$^+$ cations belonging to the same single layer. The isobutyl groups of the cations are located in the outer parts of the layer while the amine N atom of the cations and bromide anions lie in its internal part (see Figure 1-right). At 293 K, bromide anions are

---

Dr. A. Piecha-Bisiorek, Dr. A. Białońska,
Prof. R. Jakubas, M. Wojciechowska
Faculty of Chemistry
University of Wrocław
F. Joliot-Curie 14, 50-383 Wrocław, Poland
E-mail: anna.piecha@chem.uni.wroc.pl
Prof. P. Zieliński, Dr. M. Gałązka
The H. Niewodniczański Institute
of Nuclear Physics
PAN
ul. Radzikowskiego 152, 31-342 Kraków, Poland

DOI: 10.1002/adma.201501812

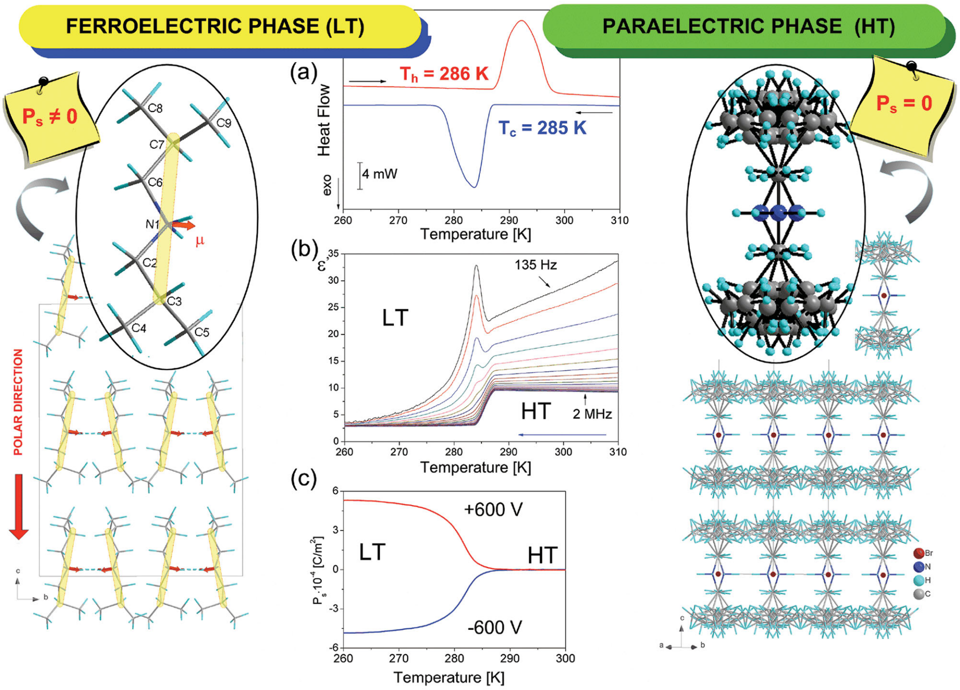

Figure 1. Molecular structure and packing of the DIBAB in the paraelectric phase at 293 K (right) and in the ferroelectric phase at 100 K (left) together with (a) DSC curves for the DIBAB compound; (b) Temperature dependence of the real part (ε') of the complex dielectric constant measured in the cooling mode between 135 Hz and 2 MHz along the *c*-direction; (c) Ferroelectric properties of DIBAB–temperature dependence of the spontaneous polarization estimated from the pyroelectric current measurements.

separated from the amine N atom of the disordered cations by distances of 3.489 and 4.289 Å.

Below 285 K, the symmetry of DIBAB changes to the orthorhombic *Iba*2 space group. The orientation of the axes *a* and *b* of the unit cell in the low-temperature (LT) phase corresponds to the square diagonals of the unit cell of the high-temperature (HT) phase (see **Figure 2**). Additionally, in the LT phase, the lattice constant *b* is doubled. Every atom in the LT phase is located in a general position. As at room temperature (HT phase), in the LT phase the ions are assembled into layers, here parallel to the (001) plane. However, in the LT phase, the single layer is built up of separated hydrogen bonded zig-zag chains extended along the [100] direction. In the zig-zag chains, the amine N atom of DIBA$^+$ cations donates to two N—H$^+$···Br$^-$ hydrogen bonds. The neighboring hydrogen bonded chains along the [010] direction are oriented antiparallel (see **Figure 3**b).

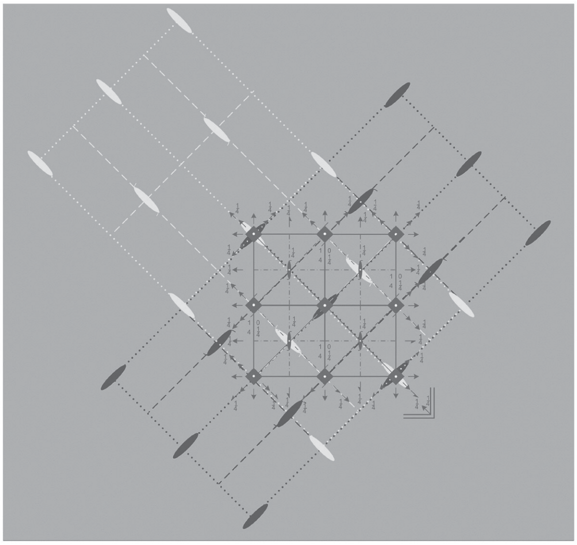

Figure 2. Relation between orientation of the unit cell before and after the phase transition and distribution of symmetry operators in paraelectric (green) and ferroelectric phases (blue or yellow).

All the N and Br atoms of the chain are located in the same plane perpendicular to the [001] direction. However, the cations do not protrude quite perpendicularly to the plane (see Figure 1-left). The angle (p_{HB}-p_+) between the plane of the ···H—N—H$^+$···Br$^-$··· chain (p_{HB}) and the plane of the cation (defined by the C2, N1, and C6 atoms) (p_+) is equal to 81.9(7)°, and the angles between the planes (p_+) of the neighboring cations (i) in the hydrogen bonded chain (p_+-p_+(0.5+*x*, 1.5–*y*, *z*)) and (ii) between the consecutive chains of the layer (p_+-p_+(1–*x*, 1–*y*, *z*)) are equal to 77.1(8)° and 16.2(17)°, respectively. As a result, the vectors of the dipole moments are neither parallel nor perpendicular to the ···H—N—H$^+$···Br$^-$··· chain, but are all directed outwards and slightly inclined towards the *c*-axis (see red arrows in Figure 1-left) so that there is a net dipole moment in the [001] direction (see also Figure S4, Supporting Information). This gives rise to a weak spontaneous polarization in a close analogy to canted magnetism.[28]

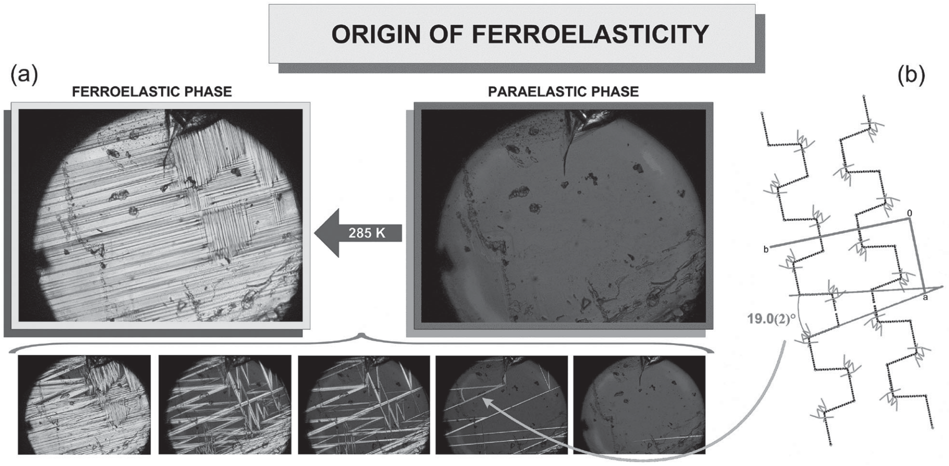

Figure 3. a) Evolution of the ferroelastic domain pattern (see also films F1 and F2) and its relation with the hydrogen bond geometry; b) packing of crankshaft-shaped molecular chains in the LT phase.

The polar properties of DIBAB in the LT phase have been studied by the pyroelectric current measurements (more details in Supporting Information). As it is seen in Figure 1c the spontaneous polarization (P_s) was found to be reversible in an external electric dc field (±6 kV cm^{-1}). The value of P_s is rather small in comparison to diisopropylammonium analogues DIPAC and DIPAB, and equals 5×10^{-2} μC cm^{-2}. This corroborates the structural findings concerning the orientation of molecular permanent dipoles. The behavior of the spontaneous polarization also resembles that of a canted ferromagnetism.[28]

The ordering mechanism responsible for the transformation of the structure is presented in Figure 1-right and -left. Zig-zag shaped, hydrogen-bonded molecular chains arise and order approximately in the [001] direction with, however, a certain slanting angle. The distance of the chains in the [010] direction diminishes significantly, which explains a 7.5% collapse of the lattice constant *b* in the LT phase.

The dynamics of the diisobutylammonium cations in LT and HT phases is reflected in the dielectric measurements. As is presented in Figure 1b the real part of the complex dielectric constant shows an abrupt anomaly, which starts at 285 K during a cooling cycle. However, the dielectric response evolves with increasing frequency. In the low-frequency range (between 135 Hz and 3 kHz) the curve ε' vs. temperature shows a strong peak (at ≈282 K), which continuously decreases with frequency. It is also noteworthy that the maxima of the low-frequency peaks appear exactly at the same temperature (282 K) as the end of dielectric anomalies for higher frequencies. However, no relaxation process was detected in the vicinity of the phase transition. Atypical dielectric behavior below room temperature reflects the complicated mechanism of this transition where the strong spontaneous deformation is a secondary effect of a molecular ordering and the canted ferroelectricity is only a residual symptom of antiferroelectric arrangement of molecular dipoles. In view of the unit cell quadrupling the ferroelectricity should be classified as improper (see also Figure S5 and S6, Supporting Information).[29–31]

Formation and packing of the hydrogen-bonded zig-zag chains in the LT phase leads to a huge deformation of the crystal lattice with respect to the HT phase. In the HT phase, all the bromide anions are located in mutually perpendicular (110) and (–110) planes, and the nitrogen atoms of the disordered cations are deviated from the planes. The interplanar distance between (110) or (–110) planes in the HT phase is equal to 3.868(2) Å. In the LT phase, the nitrogen atoms of the ordered cations of the neighboring, antiparallel oriented chains lie approximately in the corresponding planes (perpendicular to the [100] and [010] directions in the LT phase), and bromide anions lie in the ones of the corresponding planes (perpendicular to the [010] direction) and are deviated from the other. In the LT phase, the distances between the anionic planes perpendicular to the [010] direction determine the width of the hydrogen-bonded zig-zag chain and the length separating the neighboring chains in the layer. The distances are equal to 3.223(5) and 4.011(6) Å, respectively, which are 0.645 Å shorter and 0.143 Å longer than the corresponding distances in the HT phase (the distance between the (110) or (–110) planes is equal to 3.868(2) Å). As mentioned above, in the LT phase, the amine N atoms of cations lie (approximately) in the planes perpendicular to the [100] direction, and the bromide anions are deviated from the planes. The N—Br vectors are directed outwards on both sides of the planes and the angle between the N—Br vectors directed outwards on opposite sides of the plane is equal to 19.0(2)°. It is interesting that the angle 19.0(2)° is very close to that observed between certain phase boundaries when the LT phase grows at the expense of the initial tetragonal phase (see Figure 3 and Figure S7, Supporting Information).

The lattice constant *b* collapses by about 7.5% giving a rise to a strong macroscopic deformation. Nevertheless, the ferroelasticity is formally improper in this case[32] and the strain is, still formally, a secondary effect.

An insight into the space groups *I*4/*mmm* and *Iba*2 of HT and LT phases, respectively, of DIBAB shows that they do not satisfy a group–subgroup relation in this phase transition (see Figure 2). Indeed, it is impossible to select, out of the symmetry elements of the group I4/*mmm*, the ones forming the space group *Iba*2 with the transformation matrix:[33]

$$\begin{pmatrix} 1 & 1 & 0 & q_1 \\ 2 & -2 & 0 & q_2 \\ 0 & 0 & 1 & q_3 \end{pmatrix}$$

for whatever translation vector (q_1, q_2, q_3) as follows from the crystallographic data. Such a symmetry change requires a very particular rearrangement of atoms. They must, namely, leave the positions ensuring the "lost" symmetry elements to arrive at the positions corresponding to the "gained" ones. A rearrangement of this type is attained sometimes without breaking of the lattice despite large differences in geometry and packing. A condition for this is that a plane in the parent phase to be structurally close to a plane in the final phase. This plane then becomes a habit plane, i.e., a coherent interphase boundary. The behavior is characteristic of martensitic phase transitions[27] (see also films: F1 and F2 recorded during observation of DIBAB under polarizing microscope during cooling and heating cycles respectively and Part 6, Supporting Information). In fact the lattice constants *c* of DIBAB in both phases are very close. This also applies to the lattice constant *a* in LT phase and $a\sqrt{2}$ in HT phase (the diagonal of the base of the tetragonal structure), which are 7.776(4) Å and 7.735(2) Å, respectively. The planes (110) and (1–10) in the HT phase, parallel to the ferroelectric axis in the LT phase seem, therefore, to be good candidates for the habit planes. The evolution of the phase transition on cooling (Figure 3) corroborates this hypothesis. The new phase intrudes into the initial one in two perpendicular directions in the (001) plane and the crystal does not break. Subsequent intrusions subtend angles of about 19.08° to 20.08° with the initial intrusions. As mentioned above, the angle is very close to the one of some N—Br bonds. The resulting pattern is very similar to that described in Fe(30%)Ni alloy being a result of a system of accommodation strains.[27] When the phase transition is completed the system of the domains becomes typical of a ferroelastic species with perpendicular domain walls. This can be deduced from the Sapriel's theory[34] if we consider only the spontaneous strain accompanying the transition from a tetragonal to orthorhombic symmetry. The stress-free domain walls, would then be parallel to the base diagonals of the elementary cuboid, i.e., [110] and [1–10]. Their angle would be as different from 90° as 56.513°. In the final state of the phase transition, the domain walls are quasi perpendicular, however. This suggests that we have to take into account the deformation of the elementary square $\sqrt{2}a \times \sqrt{2}a$ disregarding the doubling of the unit cell in the *b* direction. The resulting angle is 86.864°. In contrast to the simple metallic crystals and to typical martensitic phase transitions the unit cell of DIBAB is four times larger. Therefore, the existence of antiphase domains is expected.[35] Such domains are not visible in the polarizing microscopy but may contribute to the mechanism of the nucleation and growth of the new phase.

In summary, we have successfully synthesized and presented systematic characterization of an original, environment-friendly biferroic (ferroelectric and ferroelastic) material diisobutylammonium bromide, $[\text{i-}(C_4H_9)_2NH_2^+][Br^-]$, (DIBAB). The material exhibits unique and unexpected properties related to ordering of chains of diisobutylammonium cations. It namely undergoes a strongly discontinuous phase transition driven by an order–disorder mechanism strongly coupled to macroscopic deformation. Being essentially antiferroelectric, the crystal shows a weak canted ferroelectricity. The study is, thus, an evidence of a canting ferroelectricity recently predicted in DFT calculations.[36] Despite the deformation and the nonexistence of a group–subgroup relation, the crystal preserves its integrity and shows a phase growth and a domain pattern resembling that of martensitic phase transitions. Undoubtedly, this rare example of a strong order–disorder induced ferroelasticity giving rise to a reproducible domain pattern known from martensitic phase transitions opens interesting prospects for new technological applications of ferroic crystals.

Experimental Section

Synthesis: A mixture of diisobuthylamine $[(CH_3)_2CHCH_2]_2NH$, (99%; Sigma–Aldrich) and concentrated HBr (47%–49%, J.T. Baker) were dissolved in EtOH/H_2O (1:1, v/v) solvent. The solution was slowly evaporated in 277 K creating thin petals of compounds with a thickness between 0.2–0.35 mm. Anal. calcd for $C_8H_{20}NBr$: C 45.72, H 9.59, N 6.66; found: C 45.86, H 9.79, N 6.70. The phase purity was verified by powder XRD and IR spectra (see Figure S2 and S3, Supporting Information).

Crystal Structures: DIBAB at 293 K: $C_8H_{20}NBr$, $M_r = 210.16$, Tetragonal, *I*4/*mmm*, $a = 5.470(2)$ Å, $b = 5.470(2)$ Å, $c = 19.628(3)$ Å, $V = 587.3(4)$ Å^3, $Z = 2$, $D_c = 1.188$ g cm^{-3}, R_1 ($I > 2\sigma(I)$) = 0.053, wR_2 (all data) = 0.122, $\mu = 3.448$ mm^{-1}, $S = 1.016$. DIBAB at 100 K: Orthorombic, *Iba*2, $a = 7.776(4)$ Å, $b = 14.468(15)$ Å, $c = 19.35(3)$ Å, $V = 2177(4)$ Å^3, $Z = 8$, $D_c = 1.282$ g cm^{-3}, R_1 ($I > 2\sigma(I)$) = 0.051, wR_2 (all data) = 0.152, $\mu = 3.720$ mm^{-1}, $S = 1.092$. Details concerning the crystal structure determination are in Supporting Information.[37,38]

Physical Properties Measurements: Differential scanning calorimetry (DSC) heating traces were obtained using a PerkinElmer model 8500 differential scanning calorimeter calibrated using n-heptane and indium. Hermetically sealed Al pans with the polycrystalline material were prepared in a controlled-atmosphere N_2 glovebox. The measurements were performed between 100 and 310 K. The thermal hysteresis was estimated from the scans performed at various rates (20, 10, and 5 K min^{-1}) extrapolated to a scanning rate of 0 K min^{-1}. Simultaneous thermogravimetric analysis (TGA) and differential thermal analysis (DTA) were performed on Setaram SETSYS 16/18 instrument in the temperature range 300–650 K with a ramp rate 2 K min^{-1}. The scans were performed in flowing nitrogen (flow rate: 1 dm^3 h^{-1}).

The complex dielectric permittivity, $\varepsilon^* = \varepsilon' - i\,\varepsilon''$ was measured between 100 and 310 K by the Agilent 4284A Precision LCR Meter in the frequency range between 135 Hz and 2 MHz. The overall error was less than 5%. The single-crystal samples had dimensions ca. 5 × 3 × 0.3 mm^3. Silver electrodes were sticked on the opposite faces. The dielectric measurements were carried in a controlled atmosphere (N_2) (see also Part 4 in Supporting Information). Pyroelectric current was measured by Keithley 617 Electrometer (more details in Part 5, Supporting Information). The ferroelastic domain structure of the DIBAB crystal was studied by means of an Olympus BX53 optical polarization microscope. The samples were placed in a LINKAM THM-600 heating/cooling stage, where the temperature was stabilized to within 0.1 K (Part 6, Supporting Information).

CCDC 1059278–1059279 contains the supplementary crystallographic data for this paper. These data can be obtained free of charge from The Cambridge Crystallographic Data Centre via www.ccdc.cam.ac.uk/data_request/cif.

Supporting Information

Supporting Information is available from the Wiley Online Library or from the author.

Acknowledgements

This research was supported by the National Science Centre (Poland) under grant No. 2013/11/D/ST8/03297.

Received: April 16, 2015
Revised: June 25, 2015

---

[1] J. Curie, P. Curie, *C. R. Acad. Sci. Paris* **1880**, *91*, 294.
[2] J. Valasek, *Phys. Rev.* **1921**, *17*, 475.
[3] G. Busch, P. Scherrer, *Naturwissenschaften* **1935**, *23*, 737.
[4] G. Shirane, A. Takeda, *J. Phys. Soc. Jpn.* **1952**, *7*, 5.
[5] E. Sawaguchi, *J. Phys. Soc. Jpn.* **1953**, *8*, 615.
[6] Y. Xu, *Ferroelectric Materials and Their Applications*, North-Holland, New York **1991**.
[7] K. Okazaki, *Ceramic Engineering for Dielectrics*, Zinatne, Tokio **1969**.
[8] M. N. Rahaman, *Ceramic Processing and Sintering*, Marcel Dekker, Inc., New York **1995**, p. 15.
[9] S. Horiuch, F. Ishii, R. Kumai, Y. Okimoto, H. Tachibana, N. Nagaosa, Y. Tokura, *Nat. Mater.* **2005**, *4*, 163.
[10] S. Horiuchi, Y. Tokura, *Nat. Mater.* **2008**, *7*, 357.
[11] S. Horiuchi, Y. Tokunaga, G. Giovannetti, S. Picozzi, H. Itoh, R. Shimano, R. Kumai, Y. Tokura, *Nature* **2010**, *463*, 789.
[12] A. S. Tayi, A. Kaeser, M. Matsumoto, T. Aida, S. I. Stupp, *Nat. Chem.* **2015**, *7*, 281.
[13] A. Heredia, V. Meunier, I. K. Bdikin, J. Gracio, N. Balke, S. Jesse, A. Tselev, P. K. Agarwal, B. G. Sumpter, S. V. Kalinin, A. L. Kholkin, *Adv. Funct. Mater.* **2012**, *22*, 2996.
[14] Y. Liu, Y. Zhang, M.-J. Chow, Q. N. Chen, J. Li, *Phys. Rev. Lett.* **2012**, *108*, 078103.
[15] S. Horiuchi, F. Kagawa, K. Hatahara, K. Kobayashi, R. Kumai, Y. Murakami, Y. Tokura, *Nat. Commun.* **2012**, *3*, 1308.
[16] A. Katrusiak, M. Szafrański, *Phys. Rev. Lett.* **1999**, *82*, 576.
[17] A. S. Tayi, A. K. Shveyd, A. C. -H. Sue, J. M. Szarko, B. S. Rolczynski, D. Cao, T. J. Kennedy, A. A. Sarjeant, C. L. Stern, W. F. Paxton, W. Wu, S. K. Dey, A. C. Fahrenbach, J. R. Guest, H. Mohseni, L. X. Chen, K. L. Wang, J. F. Stoddart, S. I. Stupp, *Nature* **2012**, *488*, 485.
[18] S. Horiuchi, R. Kumai, Y. Tokura, *Adv. Mater.* **2011**, *23*, 2098.
[19] D.-W. Fu, W. Zhang, H.-L. Cai, J.-Z. Ge, Y. Zhang, R.-G. Xiong, *Adv. Mater.* **2011**, *23*, 5658.
[20] D.-W. Fu, H.-L. Cai, Y. Liu, Q. Ye, W. Zhang, Y. Zhang, X.-Y. Chen, G. Giovannetti, M. Capone, J. Li, R.-G. Xiong, *Science* **2013**, *339*, 425.
[21] A. Piecha, A. Gągor, R. Jakubas, P. Szklarz, *CrystEngComm* **2013**, *15*, 940.
[22] V. K. Wadhawan, *Introduction to Ferroic Materials*, Gordon and Breach, Amsterdam **2000**.
[23] P. Toledano, M. Guennou, J. Kreisel, *Phys. Rev. B* **2014**, *89*, 134104.
[24] Y. Ivry, J. F. Scott, E. K. H. Salje, C. Durkan, *Phys. Rev.* **2012**, *B86*, 205428.
[25] Y. Ivry, C. Durkan, D. Chu, J. F. Scott, *Adv. Funct. Mater.* **2014**, *24*, 5567.
[26] Y. Ivry, D. P. Chu, C. Durkan, *Nanotechnology* **2010**, *21*, 065702.
[27] A. L. Roitburd, *Solid State Phys.* **1978**, *33*, 317.
[28] L. Tauxe, J. Gee, H. Staudigel, *J. Geophys. Res.* **1998**, *103*, 17775.
[29] V. Dvorak, *J. Phys. Soc. Jpn. Suppl.* **1970**, *28*, 252.
[30] G. Y. Lyubarskii, *The Application of Group Theory in Physics*, Gostekhizdat, Moscow **1957**, Sec. 38 (Eng. Transl., Pergamon Press, New York 1960).
[31] A. P. Levanyuk, D. G. Sannikov, *Usp. Fiz. Nauk* **1974**, *112*, 561.
[32] J.-C. Toledano, P. Toledano, *The Landau Theory of Phase Transitions*, World Scientific, Singapore **1987**.
[33] *International Tables for Crystallography Vol. A: Space-Group Symmetry*, (Ed: Th. Hahn), Springer, The Netherlands **2006**, 78.
[34] J. Sapriel, *Phys. Rev. B* **1975**, *12*, 5128.
[35] M. Guymont, *Phys. Rev. B* **1978**, *18*, 5385.
[36] D. D. Sante, A. Stroppa, P. Jain, S. Picozzi, *J. Am. Chem. Soc.* **2013**, *135*, 18126.
[37] Oxford Diffraction, CrysAlis 'RED' **2001** Wrocław, Poland Sp. z o. o.
[38] G. M. Sheldrick, *Acta Crystallogr. Sect. A.* **2008**, *64*, 112.